AMO – Advanced Modeling and Optimization, Volume 11, Number 4, 2009

INTEGRATED APPROACH FOR LIFE PREDICTION OF THERMO-FLUIDIC SYSTEMS*

O. M. Al-Habahbeh[1], D.K. Aidun[2], P. Marzocca[3], and H. Lee[4]

[1, 2, & 3] Mechanical & Aero. Eng. Dept., Clarkson University, PO Box 5725, Potsdam, NY 13699 USA

[1] Corresponding author, alhabaho@clarkson.edu, [2] daidun@clarkson.edu, [3] pmarzocc@clarkson.edu

[4] GE Energy, Aero Package Engineering, Houston, TX 77015 USA, hauhua.lee@ge.com

Keywords: Conjugate Heat Transfer, CFD Simulation, Fluid-Solid Interaction, FEM Simulation, Fatigue Life

SUMMARY

Some thermal systems involve a high degree of technical risk. Their deterioration could be induced by the flow of high temperature fluids. A high-fidelity assessment tool is presented in this work. It is based on a broad method that can deal with complex thermo-fluidic systems. These systems may involve multiple physics interactions. The procedure integrates multiple computational tools in a fashion that enables the simulation of a wide array of systems. It provides an engineering tool based on linking several existing computational packages. It is sufficiently general that it can be employed for any thermal application involving fluid flow and a solid medium. Computational Fluid Dynamics (CFD), Finite Element Method (FEM), and Fatigue tools are integrated within the proposed approach.

The CFD part of the method is first applied to an existing experimental model [Ray et al., 2000], where heat transfer coefficients are determined using CFD, and then compared to the analytically-computed coefficients. The results showed good agreement. A simple application of a cylindrical ring model is provided to clarify the process. The process starts with CFD simulation to determine the convective terms necessary for the transient FEM thermal analysis. The thermal analysis provides maximum thermal stress whereby the fatigue life of the component is estimated. Finally, the effect of varying the turbulence intensity on heat transfer coefficients, thermal stress, and life, is investigated.

NOMENCLATURE

α Coefficient of thermal expansion (K^{-1})

***AMO - Advanced Modeling and Optimization, ISSN: 1841-4311**

β	Coefficient of volumetric thermal expansion (K^{-1})
c	Constant of proportionality
D	Inner Diameter (m)
D_{mean}	Mean Diameter (mm)
ΔT	Temperature gradient ($°C$)
E	Modulus of Elasticity (MPa)
g	Acceleration of gravity (m/s^2)
Gr_D	Grashof Number
h	Convection heat transfer coefficient ($W/m^2.K$)
h_c	Heat transfer coefficient ($W/m^2 .°C$)
k_f	Thermal conductivity of the fluid ($W/m.K$)
k_a	Heat Conductivity of air ($W/m.K$)
L	Characteristic length (m)
μ	Viscosity ($Pa.s$)
Nu_D	Nusselt Number, dimensionless temperature gradient at the surface.
P	Pressure (MPa)
Pr	Prandtl number, ratio of momentum and thermal diffusivities
q_{cond}	Total heat flux from conduction (W/m^2)
q_w	Total heat flux at wall boundary (W/m^2)
Ra_D	Rayleigh Number
Re_D	Reynold's Number
ρ	Density (kg/m^3)
σ_1	First Principal Stress (MPa)
σ_2	Second Principal Stress (MPa)
σ_3	Third Principal Stress (MPa)
σ_y	Yield Stress (MPa)
$\sigma_{Thermal}$	Thermal Stress (MPa)
σ_h	Hoop stress in pipe (MPa)
t	Thickness (mm)
T_o	Specified outside boundary temperature $(°C)$
T_s	Source temperature ($°C$)
T_∞	Film temperature ($°C$)
T_w	Temperature at the wall, $(°C)$

V Velocity (m/s)

ν Kinematic viscosity (m^2/s)

υ Specific volume (m^3/kg)

ACRONYM

AHTC Air Heat Transfer Coefficient

CCL CFX Command Language

CFD Computational Fluid Dynamics

CEL CFX Expression Language

FEA Finite Element Analysis

FEM Finite Element Modeling

FSI Fluid–Solid Interaction

ID Inside Diameter

OD Outside Diameter

WHTC Water Heat Transfer Coefficient

1. INTRODUCTION

The simulation of thermal systems is useful for predicting their performance early during the design phase. This process provides data that is essential to the improvement of the design. Understanding the thermal fluid-structure interaction helps to predict the performance, improve the design, and avoid possible future failures of the system.

Various techniques for life prediction of structures were introduced in the literature. A computational approach for the lifetime assessment of structures under thermo-mechanical loading was presented by Constantinescu, (2004). The method proposed by Constantinescu, (2004) is composed of a fluid flow, a thermal and a mechanical finite element computation, as well as a final fatigue analysis. Nakaoka et al., (1996) used analytical and experimental procedures to establish a design method for thermal stress fatigue life of a plate-fin heat exchanger. However, these methods were not based on transient analysis where it could reveal higher stress than steady-state analysis. In addition, mapping of fluid loads distributions onto the model surface provides more accuracy than imposing the average values of these loads.

On the other hand, stress analysis of thermo-mechanical systems has been treated extensively by many authors, but without considering life prediction. For example, heat transfer coefficient (h) for surfaces in contact with air flow was obtained by Asghari, (2002) by running a steady-state CFD model.

The obtained coefficient (h) was used for transient analysis instead of the analytically calculated coefficient. Similarly, Bedford et al., (2004) used a CFD-based time-averaged heat transfer coefficient (h) for thermal stress analysis. They exported h over the model boundaries. h was imported into the structural Finite Element Analysis (FEA) code where a steady-state thermal analysis is performed, which accounts for non-uniform thermal loading. Lee et al., (2006) studied the structural characteristics for inlet port of a heated air breathing engine. They performed transient temperature and stress analysis by FEM for Titanium alloy and Steel. Sawyer, (1969) devised a method for transient thermal stress analysis of two joined pipes subjected to a change of fluid temperature. Fully developed laminar flow through a pipe was considered by Al-Zaharnah et al., (2000). The thermal stresses developed due to conjugate heating were analyzed. The conjugate heat transfer and thermal stress were studied numerically by Ozceyhan, (2005). The energy and governing flow equations were solved using a finite difference scheme. FEM was used to compute the thermal stress fields. Fan, (2005) focused on how to use a steady-state temperature result obtained by a CFD analysis to conduct a thermal-stress analysis with three data transfer methods (Direct Conversion Method, Surface Mapping Method and Volume Mapping Method). A thermal model was developed by Bassi et al., (2007) that generates random variables from critical parameters to create a failure surface based on a stress failure criterion.

Other authors analyzed thermal stresses for systems not involving fluids. FEM was used by Satyamurthy et al., (1980) to calculate the transient thermal stresses in a long cylinder resulting from convective heat transfer. Huseyin and Gamze, (2005) calculated the transient temperature and thermally induced stress distributions in a rotating hollow disk.

Significant amount of work was performed on heat transfer without the structural analysis. Heat transfer associated with forced convection flow was investigated analytically and numerically by Vynnycky et al., (1998). Both internal and external thermal conductivities were taken into consideration by means of a conjugate model consisting of both the fluid and the slab. Full Navier-Stokes equations were used for the fluid medium and the energy equations were used for both the fluid and the slab. The analysis facilitates the investigation of the effects of various parameters on the heat transfer characteristics. Segarra et al., (2002) focused on the detailed analysis of some specific parts of fin-and-tube heat exchangers using CFD methodologies. They studied the quality of the numerical solutions by mesh refinement and convergence index.

It was shown by Boyce et. al., (2004) that a thermo-mechanical study considering only the steady-state operation and not considering the pulsed heating effects is insufficient. Therefore, additional study is necessary to consider the pulsed heating effects in the form of additional stress. Thermal shock shares many characteristics with thermally-induced stress, except that its behavior is time dependent as

well as spatially dependent. LeMasters, (2004) explained that during the operation of a thermal system, the rapid start-up and shut-down leads to a large temperature difference between the surface of a material and the mean body temperature. If the surface is much cooler than the body, the surface is in a state of tension. For rapid heating, the surface is in a state of compression. Since tension leads to crack growth, and heating to crack closure, rapid cooling is more severe than heating.

Because walls do not exhibit uniform temperature, performing analytical calculation of h from the Nusselt number would result in erroneous calculation. Nusselt number is interpreted as the dimensionless temperature gradient at the surface, and is defined as [Incropera, 2002]:

$$Nu_L = \frac{hL}{k_f} \tag{1}$$

where h is convection heat transfer coefficient in $W/m^2.K$, L is characteristic length in m and k_f is thermal conductivity of the fluid in $W/m.K$. [Incropera, 2002]

While fatigue life can be determined by testing a sample of the product, it is far more cost-effective to predict it during the design phase. Many authors have dealt with life assessment of mechanical systems from different perspectives, and for different applications. However, they have either been limited to single domain problems (i.e. not involving multiple domains such as fluid-structure interaction), or they haven't considered transient analysis, which could result in more stress. So there is a lack of a broad life-assessment method that can treat complex systems involving multiple physics interactions. These complex systems can't be accurately investigated using analytical formulations due to their complexity. This work combines multidisciplinary computational packages to create a practical engineering tool [Al-Habahbeh, 2008]. The tool ensures more accurate and flexible analysis for complex thermal systems by employing physics-based modeling in addition to a powerful interface that minimizes manual intervention. This leads to a robust and practical life-prediction tool. The tool can be used for a wide range of thermal systems. Although it is designed to address a specific industrial need, it is capable of modeling a wide variety of different fluid-solid combinations to find thermal stresses and fatigue life.

The CFD analysis part of the method is first applied to an experimental model [Ray et al., 2000], where the convention heat transfer coefficients are determined, and then compared to the analytically-calculated ones. The two methods showed good agreement. A simple cylindrical ring model is presented to demonstrate the proposed procedure. It is simulated using CFD and FEM, where the working fluids are water and air. The CFD simulation focuses on the three domains; water, ring, and air, which are modeled as a conjugate heat transfer problem. The cylindrical ring is built as shown in Fig. 1, with the dimensions shown in Table 3. CFD analysis is conducted on the model, and heat transfer coefficients are obtained for the steady-state and the transient cases. Generally, heat transfer coefficients can be assumed constant and

uniform during transient analysis. The FEM simulation includes using the CFD results as inputs for the FEM model, and obtaining structural thermal stresses. These stresses are used to conduct a fatigue analysis to predict the expected life of the model. The accuracies of the CFD and FEM solutions are verified by refining their respective grids three times. Thermal stress occurs because of temperature gradients that develop in the ring as a result of heat flux. The relationship between turbulence intensity and several variables is investigated. It is found that higher turbulence induces higher heat transfer coefficients and higher thermal stress, while it reduces expected life of the model.

2. CALCULATION OF HEAT TRANSFER COEFFICIENTS

A CFD simulation is performed for an existing model [Ray et al., 2000], where the CFD-computed heat transfer coefficients are compared to those computed analytically. The data cited from the experimental reference [Ray et al., 2000] is shown in Table 1.

Table 1: Experimental Data [Ray et al., 2000]

Tested Pipe	Boiler Capacity (*ton steam/hour*)	Steam State	Pipe Outer Diameter (*OD*) (*m*)	Pipe Inner Diameter (*ID*) (*m*)	Pipe Average Wall Thickness (*t*) (*m*)	Length of Pipe for Investigation (*m*)
Boiler pipe A	240	Superheated	0.273	0.227	0.023	0.45

2.1. INITIAL CALCULATIONS

Hoop stress in pipe is defined as:

$$(\sigma_h) = \frac{PD_{mean}}{2t} \tag{2}$$

where P is the pressure in MPa, D_{mean} is the mean diameter in mm and t is the thickness in mm. The resulting stress using equation (2) represents only the stress due to internal pressure. However, additional stress could result from the transient temperature gradient across the pipe. The current method takes these effects into consideration. To start the CFD part of the current method, the flow regime must be determined, and therefore Reynold's number (Re) is calculated as:

$$\mathrm{Re}_D = \frac{\rho V D}{\mu} \tag{3}$$

At a temperature of 500 °C, steam density (ρ) = 90.5 kg/m^3 (Rolle, 1999) and viscosity (μ) = 3e-5 $Pa.s$ (Steam). Boiler capacity is 240 ton steam/hour, which equals 0.737 m^3 steam/s. Since D_{mean} = 0.25 m, the pipe cross sectional area is as 0.040471 m^2. Therefore, the velocity (V) = 18.2 m/s and Re = 1.25E+07. This is much higher than 4000, so the steam flow is highly turbulent.

2.2. CFD SIMULATION BASED ON THE EXPERIMENTAL DATA

The mesh used for the CFD simulation is shown in Fig. 1. It contains the domains of the pipe, inner steam, and outer air. This model is identical to the experimental model [Ray et al., 2000].

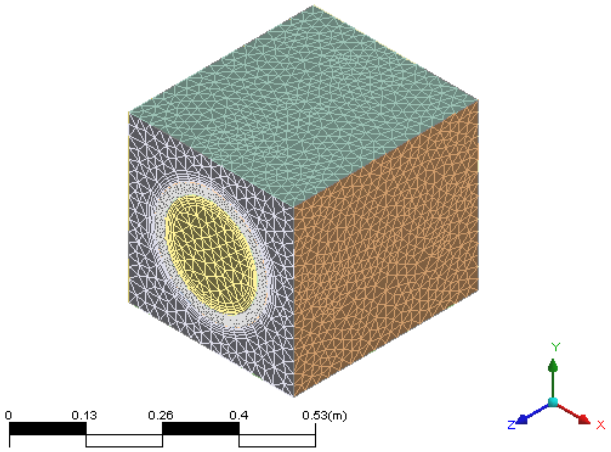

Fig. 1: CFD Mesh for Pipe, Inner Steam, and Outer Air

The CFD mesh data is shown in Table 2.

Table 2: CFD Mesh Data

Nodes	346,900
Tetrahedral	1,349,117
Pyramids	8,893
Prisms	160,967
Total number of elements	1,518,977

The CFD boundary conditions are identical to the experimental reference [Ray et al., 2000]. They are imposed on the model as shown in Fig. 2, where steam flows inside the pipe which is surrounded by still air.

As a result of CFD simulation, steam and air heat transfer coefficients are obtained as shown in Fig. 3 and Fig. 4. The average steam (inner) heat transfer coefficient is 6741 $W/m^2.K$, and the average air (outer) heat transfer coefficient is 17.5 $W/m^2.K$.

2.3. CFX METHOD FOR COMPUTING HEAT TRANSFER COEFFICIENT [ANSYS]:

The heat flux at a wall boundary is implicitly specified using an external heat transfer coefficient, h_c, and an outside or external boundary temperature, T_o. This boundary condition can be used to model thermal resistance outside the computational domain. The heat flux at the Heat Transfer Coefficient wall is calculated using:

$$q_w = h_c \left(T_0 - T_w\right) = q_{cond} \tag{4}$$

where q_w is the total heat flux at wall boundary in W/m^2, h_c is the heat transfer coefficient in $W/m^2.°C$, T_o is the specified outside boundary temperature in $°C$, T_w is the temperature at the wall (edge of the domain) in $°C$ and q_{cond} is the total heat flux from conduction in W/m^2. For turbulent flows, T_w is calculated from a surface energy balance, and for laminar flows, it is the boundary temperature field calculated by the solver.

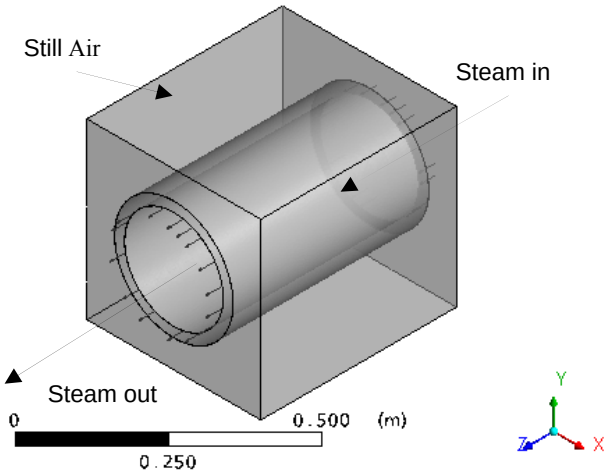

Fig. 2: Boundary Conditions on the CFD Model

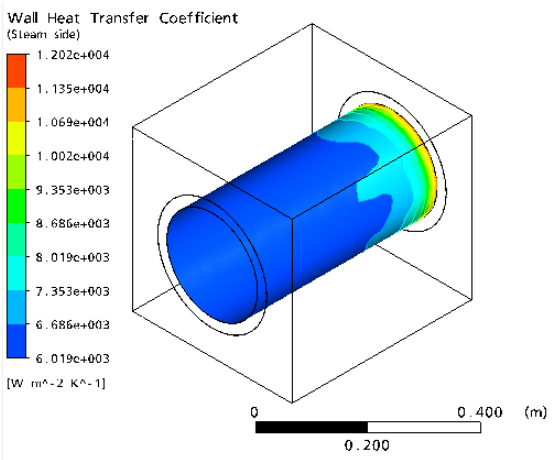

Fig. 3: Heat Transfer Coefficient Distribution of Steam Inside the Pipe

2.4. ANALYTICAL CALCULATION OF HEAT TRANSFER COEFFICIENTS

2.4.1. STEAM HEAT TRANSFER COEFFICIENT

The convective heat transfer coefficient of the steam inside the pipe is calculated by [Incropera, 2002]:

$$h_c = \frac{Nu_D k_f}{ID} \tag{5}$$

where h_c is heat transfer coefficient in $W/m^2.°C$ and Nu_D is Nusselt Number, which is the dimensionless temperature gradient at the surface.

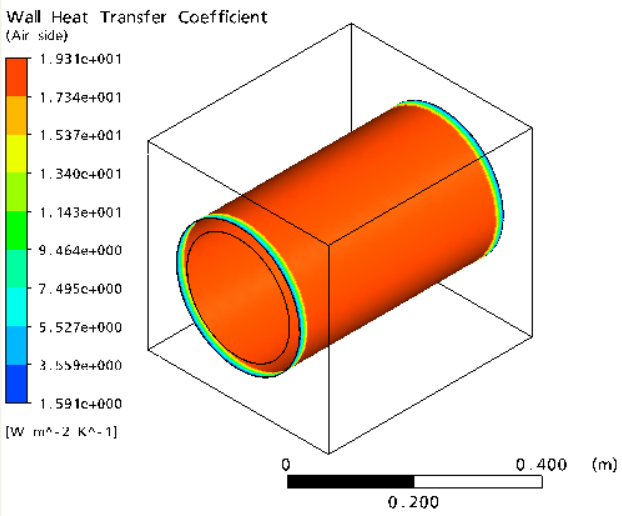

Fig. 4: Heat Transfer Coefficient Distribution of Air Outside the Pipe

For convection in turbulent flow in circular tube (internal flow), it is calculated by [Erek 2005]:

$$Nu_D = \frac{(f/2)(\mathrm{Re}-1000)\mathrm{Pr}}{1+12.7(f/2)^{1/2}\left(\mathrm{Pr}^{2/3}-1\right)} \tag{6}$$

$$f = (1.58\ln \mathrm{Re} - 3.28)^{-2} \tag{7}$$

k_f is heat conductivity of the steam (= 33.9e-3 $W/m.°C$), ID is inner diameter of the pipe (= 0.227 m) and Re_D is Reynold's number. For pipe internal flow with a temperature of 500 $°C$ and a pressure of 2.5e7 Pa, it was calculated earlier as 1.25e7. Prandtl number (Pr) is the ratio of momentum and thermal diffusivities, and equals 0.998 [Incropera, 2002]. Therefore,

$$Nu_D = 36{,}937$$

and

$$h_c = 5516\ W/m^2.°C$$

The CFD calculated h_c is 6741 $W/m^2.°C$, the difference of 18% is due to assuming uniform surface temperatures in the illustrated analytical calculation, while in reality these temperature are not perfectly uniform.

2.4.2. AIR HEAT TRANSFER COEFFICIENT

To determine air heat transfer coefficient outside the pipe, the following definition is used [Incropera,

2002]:

$$h_c = \frac{Nu_D k_a}{OD} \tag{8}$$

h_c is heat transfer coefficient ($W/m^2 .°C$), k_a is heat conductivity of air (= 26.3e-3 $W/m.°C$), OD is outer diameter of the pipe (= 0.273 m), Nu_D is Nusselt number, it is the dimensionless temperature gradient at the surface. For air free convection around a long cylinder, it is given by [Incropera, 2002]:

$$Nu_D = \left\{ 0.6 + \frac{0.387 Ra_D^{1/6}}{\left[1 + \left(0.559/\mathrm{Pr}\right)^{9/16}\right]^{8/27}} \right\}^2 \tag{9}$$

where Ra_D is Rayleigh Number, defined in equation (10) [Cengel, 2003], while Pr is Prandtl number, which is the ratio of momentum and thermal diffusivities, it equals 0.707.

$$Ra_D = Gr_D Pr \tag{10}$$

where Gr_D is Grashof Number, which is defined as [Cengel, 2003]:

$$Gr_D = \frac{g\beta\left(T_s - T_\infty\right)D^3}{v^2} \tag{11}$$

where g is acceleration of gravity (= 9.81 m/s^2), β is coefficient of volumetric thermal expansion (= 0.00327 K^{-1}), T_s is source temperature (= 498.4 °C), T_∞ is film temperature (= 33 °C), D is inner diameter (= 0.227 m) and v is kinematic viscosity (= 15.89e-6 m^2/s).

By substitution,

Gr_D = 1,203,048,915

Ra_D = 850,555,583

Therefore,

Nu = 110

h_c = 11 $W/m^2.°C$

The CFD calculated h_c is 17.5 $W/m^2.°C$, the difference of 39% is due to assuming a long cylinder while the pipe model is relatively short. Moreover, uniform surface temperatures are assumed in the analytical calculations, while in real life, they are not uniform.

3. CFD SIMULATION

After comparing the CFD results with analytical calculations, the same CFD analysis steps are applied to the cylindrical ring model. In addition, FEM and Fatigue analyses will be used to assess the life of the ring model. ANSYS/CFX® package is used for CFD simulation of the ring. The package has the

capability of solving steady-state and transient problems in thermo-fluids. It is used to simulate the fluid flow and the FSI. The basic operation of CFX® relies on utilizing control volume method, which enables a high fidelity CFD simulation of the conjugate heat transfer model. The general post-processing capabilities are used to define parameters and variables of interest to this work, such as average heat transfer coefficients.

The procedure used for this model can be applied for more complicated thermal models. The simulation process includes building a CFD model and obtaining heat transfer film coefficients. The CFD simulation determines the convection heat transfer coefficients for water inside the ring and for air outside the ring, while the only mode of heat transfer across the ring is conduction. This method can be used to study similar problems in thermal components such as ducts and heat exchanger shells. The accuracy of the solution is verified by refining the grid multiple times.

The conducted analyses include CFD and one-way thermal FSI. The steps for conducting these analyses include building the geometry using ANSYS Workbench® Design Modeler, meshing the model using CFX®-Mesh, setting–up the model and applying boundary conditions using CFX®-Pre, solving the steady-state and transient cases using CFX®-Solver, and post-processing the results in CFX®-Post. Conjugate heat transfer is used to model heat conduction across the ring wall. The domains of the model are:

1) Water running in the ring
2) Steel Ring
3) Ambient air

Throughout the analysis, air is assumed an ideal gas, air pressure is 101.3 kPa, and water pressure is 700 kPa, while air and water inlet temperatures and water flow rate are variable parameters. The air natural convection flow is assumed laminar, while k-ε turbulence model is used to describe water flow.
The boundary conditions imposed are shown in Fig. 5 and listed below:

1- Air enclosure with still air.
2- Water enters from the right side of the ring and leaves from the left side.
3- Ring inner wall, which is the interface between the ring and the water, with no slip boundary condition.
4- Ring outer wall, which is the interface between ring and air, with no slip boundary condition.
5- Temperature of air enclosure outer wall is equal to ambient air temperature.

Table 3: Model Dimensions

Dimension	Value	Unit
OD	60	cm
ID	50	"
Length	20	"

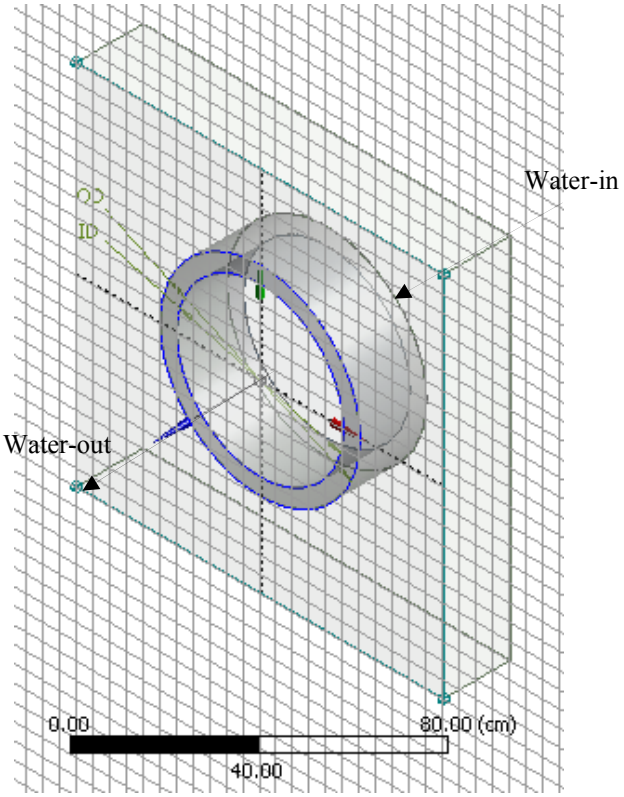

Fig. 5: Cylindrical Ring Model

The Tetrahedron finite volume element is used for meshing the model, in addition to inflation layers for boundary layer refinement, and face proximity to achieve the required number of elements across the ring thickness. Fig. 6 shows part of the finite volume mesh. The mesh contains around 326,000 tetrahedron and prisms elements.

The grid is verified by using three different mesh sizes. Table 4 shows the mesh sensitivity in terms of air and water heat transfer coefficients.

Table 4: CFD Mesh Sensitivity

Mesh Size (No. of Elements)	Error in AHTC (%)	Error in WHTC (%)
124,119	0.14	0.02
138,679	0.11	0.08
203,357	0.07	0.00

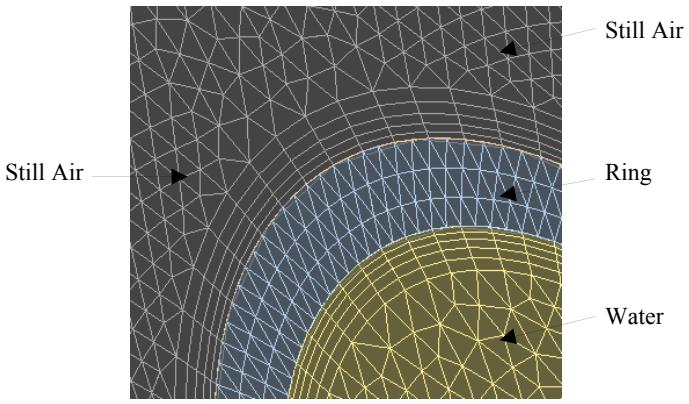

Fig. 6: Finite Volume Mesh

From Table 4, it can be seen that a reasonable mesh independency is achieved using 2x2 grid. This grid size is used for all subsequent CFD analyses.

Once the CFD data is available, it is used as input to the FEM transient analysis.

3.1. USING PARAMETERS AND EXPRESSIONS IN ANSYS/CFX®

In order to define the CFD input and output parameters, CFX Expression Language (CEL) and CFX Command Language (CCL) are used. CEL is used to define response quantities such as average temperatures of areas and volumes, while CCL is used to define input parameters in CFX®.

3.2. CFD INPUT DATA

The CFD input data used for this analysis are listed in Table 5. Reynolds number (*Re*) for water is calculated as 3,217,733 which is highly turbulent.

Table 5: CFD Input Data

Air Temp. (°C)	Water Flow Rate (kg/s)	Water Temp. (°C)	Water Density (kg/m^3)	Water Velocity (m/s)	Water Viscosity (Pa.s)
15	400	90	965.3	2.1	3.15e-4

3.3. CFD RESULTS

As a result of the CFD analysis, heat transfer coefficients for water and air are shown in Fig. 7 and 8,

respectively. The results of the CFD analysis are summarized in Table 6.

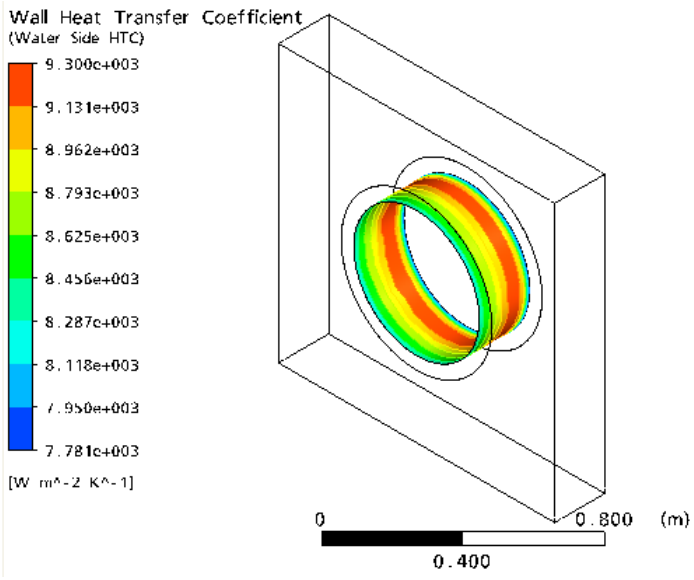

Fig. 7: Water Heat Transfer Coefficient

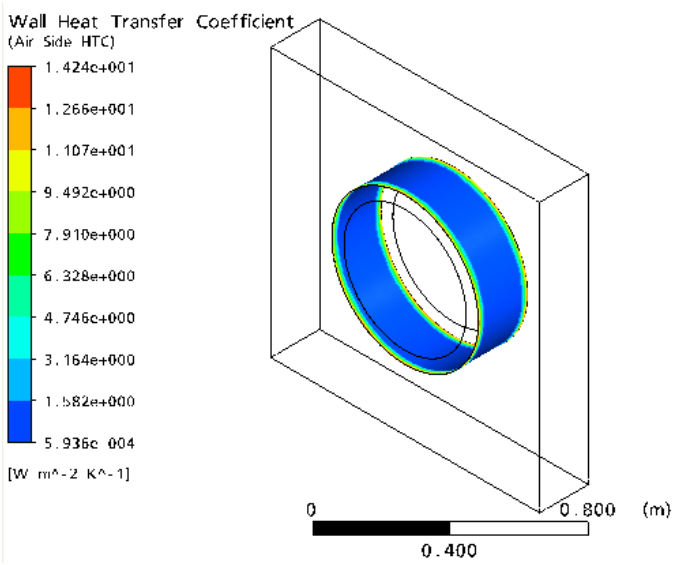

Fig. 8: Air Heat Transfer Coefficient

Table 6: CFD Output Data

Parameter	Air HTC (W/m^2 °C)	Water HTC (W/m^2 °C)
Area average value	0.001	8617

4. FEM MODELING

The CFD results are used for FEM analysis to obtain thermal stresses. These stresses cause cyclic thermal fatigue; therefore, they are identified as the cause of failure. Some of the potential factors that may control thermal stress are:

1- Water temperature and flow rate
2- Ring dimensions
3- Ambient air temperature

Since the transient thermal stress due to start-up operation is expected to be more critical than the steady-state stress, it should be the basis for the fatigue life evaluation. The stress is developed in the model due to temperature gradient which results from heat flux. In order to determine the maximum stress, the system is modeled using transient thermal analysis, whereby structural analyses are conducted over multiple periods of time to determine the maximum stress value.

To determine the max thermal stress, the CFD results are imposed onto a corresponding FEM model in ANSYS Simulation®, a transient FEM simulation is set-up at regular intervals up to the steady-state. A fatigue analysis is conducted to estimate the life of the ring model. Steady-state is reached approximately at time = 625 sec. The calculated stresses include von-Mises and maximum shear stress. Von-Mises failure criterion is defined as [Hosford, 2005]:

$$\left(\sigma_1-\sigma_2\right)^2+\left(\sigma_2-\sigma_3\right)^2+\left(\sigma_1-\sigma_3\right)^2\le 2{\sigma_y}^2 \tag{12}$$

where σ_1, σ_2, and σ_3 are the principal stresses, and σ_y is the yield stress for the ductile material.

Thermal stress $\sigma_{Thermal}$ is generally expressed in the form [NEA, 1998]:

$$\sigma_{Thermal}=c.E.\alpha.\Delta T \tag{13}$$

The factors that affect thermal stress are E which is Modulus of Elasticity (*MPa*), α which is coefficient of thermal expansion ($°C^{-1}$), ΔT which is temperature gradient ($°C$) and c which is a constant of proportionality. The constant depends on the condition of mechanical constraint, temperature distribution, and Poisson's ratio.

The value of the maximum stress is used to predict the ring model life based on fatigue analysis. Thermal stress has more effect on service life than mechanical stress. The effect can be as much as 2.5 percent lower cycles [Oberg]. This factor is integrated into the results of this analysis.

The mesh used for the FEM analysis is shown in Fig. 9. It consists of more than 9000 hexahedral elements. The grid was refined three times in order to reach acceptable mesh independency, as shown in Table 7.

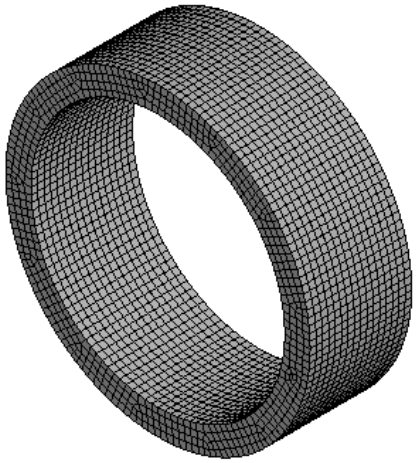

Fig. 9: Fem Hexahedral Mesh

In Table 7, a very low error is reached for a thermal load of 41 $°C$ at the inside wall of the ring. This indicates that the results are mesh-independent. Table 8 shows input data used for the FEM analysis. Once a good mesh is obtained, FEM simulation is started.

Table 7: Mesh Sensitivity

Mesh	Max Stress (*MPa*)	Error
Coarse	9.72	---
Medium	9.63	-0.01
Fine	9.62	-0.001

Table 8: FEM Input Data

Air Temp. (°*C*)	Water Temp. (°*C*)	ID (*cm*)	OD (*cm*)
15	90	50	60

Thermal stress analysis is based on transient analysis rather than steady-state, because the latter usually underestimates its value [Boyce, 2004]. Therefore, the first step is to define a transient thermal analysis, which is used to conduct the structural analysis. It is worth noting that it is not known in advance when the maximum stress occurs, therefore it is necessary to investigate the whole transient period to find the maximum stress value. The FEM thermal analysis is conducted at regular intervals for a time period of 500 s as shown in Fig. 10.

4.1. FEM RESULTS

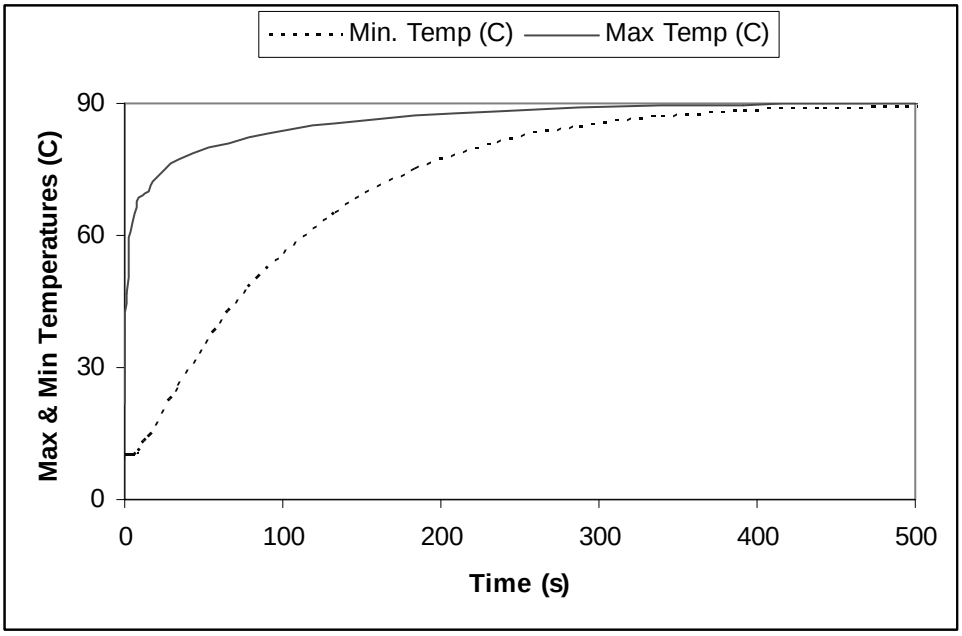

Fig. 10: Max & Min Temperatures

The transient thermal analysis is shown in Fig. 10 for a range of 500 seconds. The two lines represent the minimum and maximum temperatures within the body. They indicate the thermal gradient which is responsible for thermal stress. The maximum thermal stress is calculated for regular intervals within the transient regime and plotted against time in Fig. 11, it occurs at 8.75 s

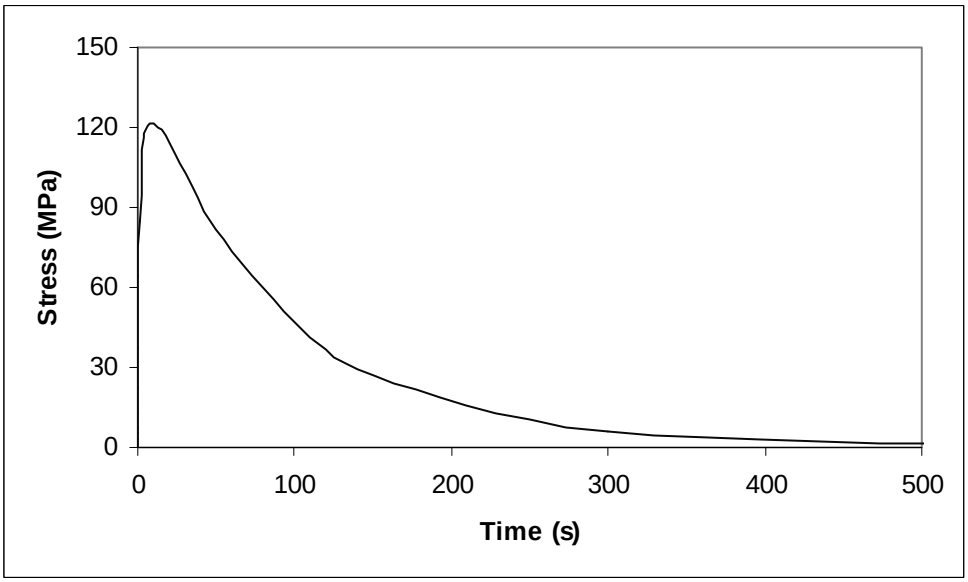

Fig. 11: Max Transient Thermal Stress

The temperature distribution corresponding to the maximum stress is shown in Fig. 12 and the maximum thermal stress distribution at 8.75 s is shown in Fig. 13. The highest stress is in the inner wall of the ring, induced by expansion due to higher temperature of the water.

Based on the maximum thermal stress, fatigue life is calculated using the material *S-N* curve and the fatigue module provided in ANSYS Simulation®. The fatigue life distribution is shown in Fig. 14. A summary of the FEM and fatigue output data is shown in Table 9.

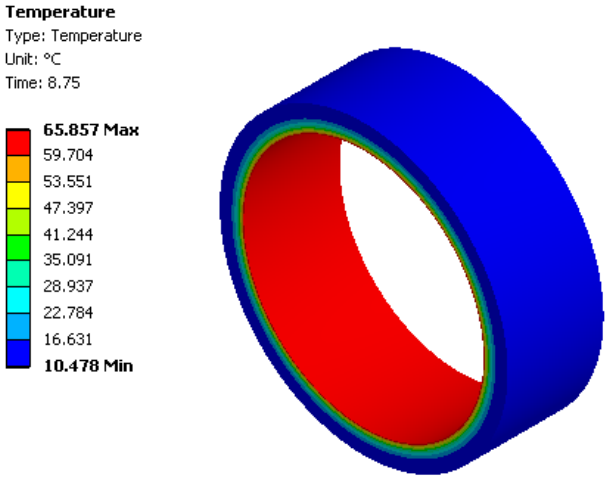

Fig. 12: Transient Temperature Distribution

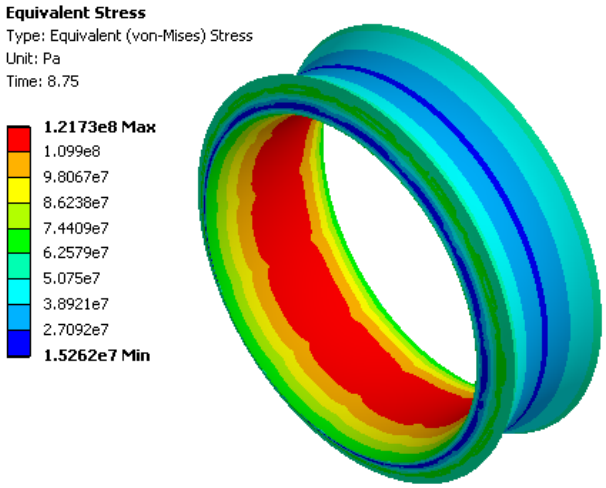

Fig. 13: Max Thermal Stress Distribution

Table 9: FEM Output Data

Max. Temp. (°C)	Equivalent Stress Max. (*MPa*)	Life (*Years*)
65.9	121.7	15.4

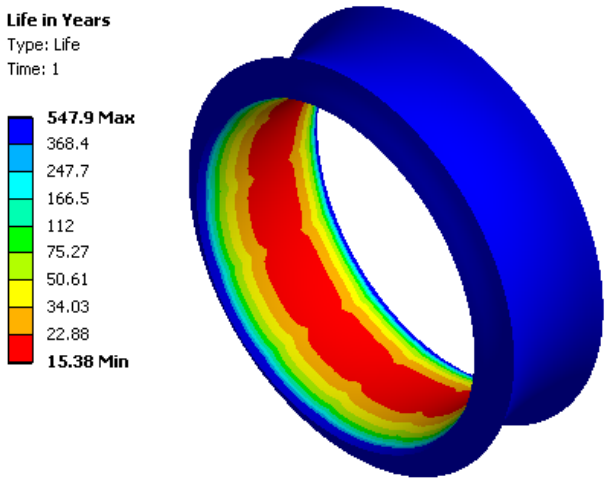

Fig. 14: Fatigue Life Distribution

5. EFFECT OF FLOW TURBULENCE ON LIFE

As flow velocity may change, so the turbulence level. That would affect the life of the ring. To investigate this issue further, fatigue life is calculated for different turbulence levels. Three turbulence levels are investigated, and the results are shown in Table 10 and Figures 15-17. It is found that the higher the flow turbulence, the higher the heat transfer coefficient as shown in Fig.15. Fig. 16 shows that the thermal stress increases with turbulence as well. Fig. 17 shows that as the flow turbulence increases, life decreases. These simulations provide information that could help in planning more frequent maintenance or inspection in cases where higher turbulence is expected.

Table 10: Turbulence Effect

Turbulence Intensity (%)	1	5	10
Water Heat Transfer Coefficient ($W/m^2.K$)	8201	8617	9547
von-Mises Stress (*MPa*)	121	123	127
Life (*Years*)	15.9	14.6	12.5

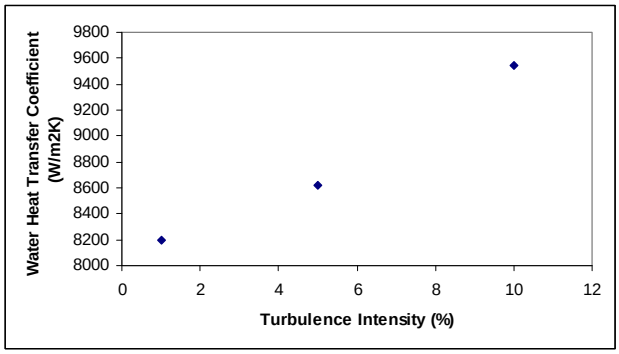

Fig. 15: Turbulence Effect on Heat Transfer Coefficient

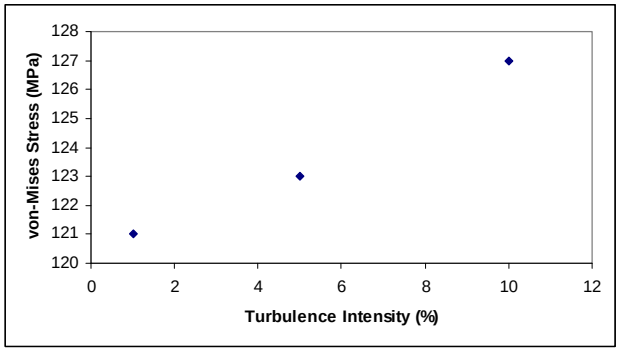

Fig. 16: Turbulence Effect on Thermal Stress

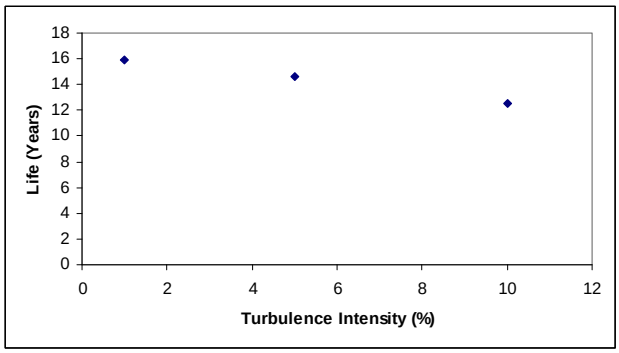

Fig. 17: Turbulence Effect on Life

6. CONCLUSIONS

The heat flux between the inner and outer fluids creates temperature gradients in the structure, which cause thermal stresses that affect component life. The maximum thermal stress should be based on transient analysis and not steady-state, because the thermal gradients in the transient case are much higher than the ones in the steady-state.

The thermal stress approaches zero after the model reaches steady-state. Since the temperature gradient (the difference between maximum and minimum temperatures) also approaches zero. This relationship is evident by looking at figures 10 and 11.

CFD analysis can be used to determine wall heat transfer coefficients, thereby eliminating the need for analytical calculation which is not possible for complex geometries. However, for this simple geometry, analytical calculations of the heat transfer coefficients were conducted, and compared to the CFD results. The differences are due to the assumptions of the analytical calculation. Finally, the effect of turbulence on the heat transfer coefficients and the thermal stress is investigated and found directly proportional, while the effect of turbulence on life is found inversely proportional which may warrants more frequent inspections.

ACKNOWLEDGMENT

The authors would like to acknowledge support for this research provided by GE Energy, Houston, TX.

REFERENCES

[1] Al-Habahbeh O.M., Aidun D.K., Marzocca P., and Lee H., (2008) Evaluation of Heat Transfer Effect on a Thermal System Using Numerical Simulation, IMECE2008-68368, *Proceedings of ASME International Mechanical Engineering Congress and Exposition*, Boston, MA, USA.

[2] Al-Zaharnah, I. T., Yilbas, B. S., and Hashmi, M. S. J., (2000) Conjugate heat transfer in fully developed laminar pipe flow and thermally induced stresses, *Comput. Methods Appl. Mech. Engrg.*190, pp.1091±1104.

[3] ANSYS® Reference Manuals

[4] Asghari, T.A., (2002) Transient thermal analysis takes one-tenth the time, Motorola Inc, EDN.

[5] Bassi, C., Devictor, N., Marquès, M., Nayak, A. K., and Saha, D., (2007) Progress in reliability methodology for passive systems", 4th CRP IAEA Meeting on Natural Circulation & Passive Systems Reliability. Nice, France.

[6] Bedford, F., Hu, X., and Schmidt, U., (2004) In-cylinder combustion modeling and validation using Fluent.

[7] Boyce R., Dowell, D.H., Hodgson, J., Schmerge, J.F., and Yu, N., (2004) Design Considerations for the LCLS RF Gun, Stanford Linear Accelerator Center, LCLS TN 04-4, pp.21. (http://www-ssrl.slac.stanford.edu/lcls/technotes/lcls-tn-04-4.pdf).

[8] Cengel Y.A., (2003) Heat Transfer, A Practical Approach, (2nd Edition), McGraw Hill Professional, pp.466.

[9] Constantinescu, A., Charkaluk, E., Lederer, G., and Verger, L., (2004) A computational approach to thermomechanical fatigue", *International Journal of Fatigue* V. 26 pp.805–818.

[10] Erek A., Ozerdem B., Bilir L., and Ilken Z., (2005) Effects of Geometrical Parameters on Heat Transfer and Pressure Drop Characteristics of Plate Fin and Tube Heat Exchangers, *J. Applied Thermal Engineering*, Vol. 25, pp.2431.

[11] Fan, Q. Y., (2005) Transient Thermal Flow and Thermal Stress Analysis Coupled NASTRAN and SC/Tetra", http://www.shenmo.sh.cn/industry/CFD%20Paper-6.pdf.

[12] Hosford W. F., (2005) Mechanical Behavior of Materials", ISBN 0521846706, Cambridge Press, pp.83.

[13] Hüseyin, Y., and Gamze, B., (2005) Numerical solutions of transient conjugate heat transfer and thermally induced stress distribution in a heated and rotating hollow disk", *J. Energy conversion and management*, ISSN 0196-8904, vol. 46, No. 1, pp.61-84.

[14] Incropera F.P., and Dewitt D.P., (2000) Fundamentals of Heat and Mass Transfer (Fifth Edition), John Wiley & Sons, pp.355, 491, 554.

[15] Lee, Y.S., Kim, H. S., Choi, Y. J., and Kim, J. H., (2006) Evaluation of Thermal Stress Resistance of Titanium Alloy for the Air Breathing Engine", Key Engineering Materials Vols. 321-323 pp.1381-1384, Trans Tech Publications, Switzerland.

[16] LeMasters J., (2004) Thermal Stress Analysis Of Lca-Based Solid Oxide Fuel Cells", Master's Thesis, Georgia Institute of Technology, pp.25, 104.

[17] Nakaoka, T., Nakagawa, T., Mitsuhashi, K., and Ueno, K., (1996) Evaluation of Fatigue Strength of Plate-Fin Heat Exchanger under Thermal Loading", International Conference on Pressure Vessel Technology, Volume 1, ASME.

[18] NEA Nuclear Science Committee, Nuclear Energy Agency (1998) Utilization and Reliability of High Power Proton Accelerators", Workshop proceedings, Mito, Japan, ISBN:9264170685, pp.320.

[19] Oberg, E., and McCauley, C.J., Machinery's Handbook: A Reference Book for the Mechanical Engineer, Industrial Press Inc., ISBN 0831127376, pp.207.

[20] Ozceyhan, V., (2005) Conjugate heat transfer and thermal stress analysis of wire coil inserted tubes that are heated externally with uniform heat flux", *J. Energy Conversion and Management*, V. 46, pp.1543–1559.

[21] Ray A.K., Tiwari Y.N., Sinha R.K., Chaudhuri S., and Singh R., (2000) Residual Life Prediction of Service Exposed Main Steam Pipe of Boilers in a Thermal Power Plant", *J. Engineering Failure Analysis*, V. 7, pp.359-376.

[22] Satyamurthy, K., Singh, J. P., Hasselman, D. P. H., and Kamat, M. P., (1980) Transient Thermal Stresses in Cylinders with a Square Cross Section Under Conditions of Convective Heat Transfer", *Journal of the American Ceramic Society* 63 (11-12) , 694–698.

[23] Sawyer, W. J., (1969) Transient Thermal Stress Analysis of a Pipe Junction", Master's thesis, Naval Postgraduate School Monterey Calif.

[24] Segarra, C. D. P., Lifante, C., Oliet, C., and Cadafalch, J., (2002) CFD Studies on Fin and Tube Heat Exchangers: Critical Analysis of the Numerical Solutions Reliability", Proceedings of the Third International Conference on Engineering Computational Technology, Stirling, Scotland.

[25] Vynnycky, M., Kimura, S., Kanev, K., and Pop, I., (1998) Forced convection heat transfer from a flat plate: the conjugate problem", *Int J. Heat Mass Transfer*. Vol. 41, No. 1. pp.45-59.